Virologica Sinica 37 (2022) 331–340

Contents lists available at ScienceDirect

Virologica Sinica

journal homepage: www.keaipublishing.com/en/journals/virologica-sinica
www.virosin.org

Research Article

Analysis of severe human adenovirus infection outbreak in Guangdong Province, southern China in 2019

Wenkuan Liu [a,1], Shuyan Qiu [a,1], Li Zhang [a,1], Hongkai Wu [a], Xingui Tian [a], Xiao Li [a], Duo Xu [a], Jing Dai [a], Shujun Gu [a], Qian Liu [b,*], Dehui Chen [a,*], Rong Zhou [a,c,*]

[a] State Key Laboratory of Respiratory Diseases, National Clinical Research Center for Respiratory Disease, Guangdong-Hong Kong-Macao Joint Laboratory of Respiratory Infectious Disease, The First Affiliated Hospital of Guangzhou Medical University, Guangzhou Institute of Respiratory Health, Guangzhou Medical University, Guangzhou, 510040, China
[b] Scientific Research Center, The First Affiliated Hospital of Guangdong Pharmaceutical University, Guangzhou, 510062, China
[c] Bioland Laboratory, Guangzhou Laboratory, Guangzhou, 510320, China

ARTICLE INFO

Keywords:
Human adenovirus (HAdV)
Human adenovirus type 7 (HAdV-7)
Severe illness
Epidemiology
Acute respiratory illness
Virulence and infectivity
Risk factor

ABSTRACT

During 2018–2019, a severe human adenovirus (HAdV) infection outbreak occurred in southern China. Here, we screened 18 respiratory pathogens in 1704 children (≤ 14 years old) hospitalized with acute respiratory illness in Guangzhou, China, in 2019. In total, 151 patients had positive HAdV test results; 34.4% (52/151) of them exhibited severe illness. HAdV infection occurred throughout the year, with a peak in summer. The median patient age was 3.0 (interquartile range: 1.1–5.0) years. Patients with severe HAdV infection exhibited increases in 12 clinical indexes ($P \leq 0.019$) and decreases in four indexes ($P \leq 0.007$), compared with patients exhibiting non-severe infection. No significant differences were found in age or sex distribution according to HAdV infection severity ($P > 0.05$); however, the distributions of comorbid disease and HAdV co-infection differed according to HAdV infection severity ($P < 0.05$). The main epidemic types were HAdV-3 (47.0%, 71/151) and HAdV-7 (46.4%, 70/151). However, the severe illness rate was significantly higher in patients with HAdV-7 (51.4%) than in patients with HAdV-3 (19.7%) and other types of HAdV (20%) ($P < 0.001$). Sequencing analysis of genomes/capsid genes of 13 HAdV-7 isolates revealed high similarity to previous Chinese isolates. A representative HAdV-7 isolate exhibited a similar proliferation curve to the curve described for the epidemic HAdV-3 strain Guangzhou01 (accession no. DQ099432) ($P > 0.05$); the HAdV-7 isolate exhibited stronger virulence and infectivity, compared with HAdV-3 ($P < 0.001$). Overall, comorbid disease, HAdV co-infection, and high virulence and infectivity of HAdV-7 were critical risk factors for severe HAdV infection; these data can facilitate treatment, control, and prevention of HAdV infection.

1. Introduction

Humans are constantly under attack by various new and old viruses (Paules et al., 2017). Some viruses [e.g., severe acute respiratory syndrome coronavirus 2 (Wiersinga et al., 2020; Zhu et al., 2020) or influenza A virus (infA) (del Rio and Guarner, 2010)] have led to global pandemics; others [e.g., human adenoviruses (HAdVs)] have mainly caused regional epidemics (Lynch and Kajon, 2016; Greber and Flatt, 2019).

HAdVs are non-enveloped, double-stranded DNA viruses of the family *Adenoviridae*. More than 100 genotypes of HAdVs have been identified and classified into seven species (A–G) (Ismail et al., 2018; Ji et al., 2021). HAdVs are associated with a broad spectrum of clinical diseases, such as acute respiratory illness (ARI), gastrointestinal infections, conjunctivitis, and obesity (Sandkovsky et al., 2014; Radke and Cook, 2018; Chen et al., 2020; Ji et al., 2021). Members of species B (e.g., HAdV types 3, -7, -14, and -55), -C5, and -E4 comprise the most common causes of respiratory disease outbreaks (Scott et al., 2016; Prusinkiewicz and Mymryk, 2019; Zhang et al., 2019).

In 2018–2019, the incidence of HAdV infection substantially increased, causing severe illness and potential death in many children in China, especially in the southern regions. Accordingly, the Chinese

* Corresponding authors.
E-mail addresses: qianliu_ln@163.com (Q. Liu), cdh84@126.com (D. Chen), zhourong@gird.cn (R. Zhou).
[1] Wenkuan Liu, Shuyan Qiu and Li Zhang contributed equally to this work.

https://doi.org/10.1016/j.virs.2022.01.010
Received 7 July 2021; Accepted 6 December 2021
Available online 17 January 2022

Center for Disease Control and Prevention issued a series of guidelines for the prevention and control of HAdV infection, as well as the diagnosis and treatment of children with HAdV pneumonia (http://www.chinacdc.cn/jkzt/crb/xcrxjb/201906/t20190628_203629.html; http://www.chinacdc.cn/kpyd2018/201906/t20190618_203285.html).

To analyze the characteristics and risk factors of this severe HAdV epidemic, we conducted a study of HAdV infection in paediatric patients hospitalized with ARI in Guangzhou, southern China in 2019. We analysed the characteristics of patients with severe HAdV infection, as well as the clinical characteristics of disease, HAdV type distribution, viral genome features, and *in vitro* viral proliferation and cytopathogenesis properties. This study was designed to provide important reference data for the treatment, control, and prevention of HAdV infection.

2. Materials and methods

2.1. Respiratory sample collection

Respiratory samples (e.g., throat swabs, sputum, and bronchoalveolar lavage fluid) from paediatric patients (≤ 14 years old, hospitalized with ARI) were collected for routine screening of respiratory viruses, *Mycoplasma pneumoniae* (MP), and *Chlamydophila pneumoniae* (CP), in accordance with established clinical protocols at the First Affiliated Hospital of Guangzhou Medical University and the First Affiliated Hospital of Guangdong Pharmaceutical University between January and December 2019 in Guangzhou, southern China (Liu et al., 2014). The samples were refrigerated at 2–8 °C in viral transport medium, transported on ice to the State Key Laboratory of Respiratory Diseases, and analysed immediately or stored at −80 °C before analysis, as previously described (Liu et al., 2014).

2.2. Respiratory pathogen screening

HAdV and 17 other common respiratory pathogens including infA, influenza B virus (infB), respiratory syncytial virus (RSV), parainfluenza virus types 1–4 (PIV1–4), human metapneumovirus (HMPV), human rhinovirus (HRV), enterovirus (EV), four types of coronaviruses (HCoV-229E, -OC43, -NL63, and -HKU1), human bocavirus (HBoV), MP, and CP were screened simultaneously using TaqMan quantitative polymerase chain reaction (qPCR), as previously reported (Liu et al., 2014).

2.3. HAdV type identification

HAdV-positive samples were subjected to further molecular typing (for HAdV-B3, -7, -14, -21, and -55, as well as -C5 and -E4) using TaqMan qPCR. Specific primers used to probe the hexon or fiber genes of HAdV are shown in Supplementary Table S1. Probe qPCR Mix (TaKaRa, RR391A, Dalian, China) was used in accordance with the manufacturer's protocol.

2.4. Clinical presentation collection

The clinical characteristics, treatments, and outcomes of patients with HAdV infections were retrospectively collected from their medical records. The diagnosis of severe or non-severe illness was identified by attending physicians, as previously reported (Dean and Florin, 2018; Pneumonia Etiology Research for Child Health Study, 2019).

2.5. Cells, HAdV-3 stock, and HAdV-7 positive sample culture

A549 cells (ATCC) were cultured in Dulbecco's modified essential medium (DMEM; Gibco, C11995500BT, Beijing, China) supplemented with 10% (v/v) foetal bovine serum (FBS; ExCell Bio, FSP500, Taicang, China) and 100 U/mL penicillin-streptomycin (Gibco, 15140–122, NY, USA); the cells were grown at 37 °C in an atmosphere of 5% (v/v) CO_2. HAdV-7-positive samples were cultured in A549 cells at 37 °C and 5% CO_2, and were then maintained under standard conditions in DMEM supplemented with 2% (v/v) FBS and 100 U/mL of penicillin-streptomycin. Inoculated cells were monitored daily for cytopathic effect (CPE); they were harvested at almost full CPE. The HAdV-3 epidemic strain Guangzhou01 (accession no. DQ099432; stored in the State Key Laboratory of Respiratory Diseases) and HAdV-7 isolates from patients with severe and non-severe illness of different durations in this study were cultured for analysis of genome features, as well as proliferation and cytopathogenesis properties.

2.6. HAdV-7 genome and capsid protein genes (hexon/penton base/fiber) sequencing and annotation

HAdV-7-positive samples were cultured and harvested for genomic or capsid protein genes (hexon/penton base/fiber) sequencing. Viral DNA was extracted using a TaKaRa Mini BEST Viral RNA/DNA Extraction Kit Ver. 5.0 (TaKaRa), in accordance with the manufacturer's instructions. Genomes were analysed by next-generation sequencing using an Illumina NovaSeq 6000 sequencer, in accordance with a protocol from Synbio-Technologies (paired-end, 2 × 150 bp). The complete genomes of HAdV-7 isolates were assembled using CLC Genomics Workbench 11.0 (Qiagen, Germantown, MD, USA). Capsid protein genes (hexon/penton base/fiber) sequencing analyses were performed via Sanger sequencing using primers shown in Supplementary Table S2. The complete genomes and hexon/penton base/fiber genes of the HAdV-7 isolates were annotated and uploaded into the GenBank database.

2.7. Phylogenetic analysis

Phylogenetic analysis was performed using Molecular Evolutionary Genetics Analysis (MEGA) version 5.05 (Tamura et al., 2011). Phylogenetic trees were constructed by the neighbour-joining (NJ) method with 1000 bootstrap replicates and default settings for all other parameters. Typical strains of HAdV species A–G sequences of genomes and hexon/penton base/fiber genes for phylogenetic analyses were retrieved from GenBank with taxon names including genome type, corresponding GenBank accession number, country of isolation, strain name, and year of isolation.

2.8. Proliferation characteristics of HAdV-7 isolates

To evaluate the proliferation characteristics of the HAdV-7 isolates in this study, HAdV qPCR was used to quantify HAdV stains. HAdV-3-Guangzhou01, a common epidemic-causing and severe pneumonia-related strain (Zhang et al., 2006), was analysed simultaneously. A549 cells (80% confluence) were infected with 0.1 mL/well of 1×10^5 copies/mL HAdV stains in 96-well culture plates at 37 °C with 5% CO_2. After virus adsorption for 2 h, the virus supernatant was aspirated and cells were washed for twice with DMEM + 2% FBS to remove unabsorbed virus. Maintenance solution (0.2 mL/well; DMEM + 2% FBS) was added for subsequent culture. A set of 2 h samples was harvested for viral genome quantification. Infected cells were then harvested at 12, 24, 36, 48, 72, 96, and 120 h post-infection; viral genome copies were quantified using adenovirus qPCR kits (Hecin, HS001, Guangzhou, China).

2.9. Viral plaque formation assay

A549 cells were seeded in six-well culture plates and incubated overnight to form dense monolayers with more than 90% confluence. After removal of the growth media, the cultures were inoculated with 0.4 mL of 10-fold serial dilutions of the viral stocks, and were then incubated for 1 h at 37 °C with rocking every 15 min. The viral inoculant was removed by aspiration and 3 mL DMEM-agarose mulch [2% SeaPlaque GTG-agarose (Lonza, 50114, Rockland, USA) mixed 1:1 with 2 × DMEM medium containing 4% FBS] was added to each well. The agarose was allowed to solidify at room temperature (20–26 °C). Plaque plates were

incubated at 37 °C and 5% CO_2 for 13 days; 1.5 mL/well of DMEM-agarose mulch was added at 4 and 8 days of incubation. Plates were stained with 2 mL/well 20% ethanol, 2% paraformaldehyde, and 1% crystal violet overnight at room temperature. The diameters of the plaques were measured using the VisionWorks software package (Analytik Jena, 8.20.17096.9551, Jena, Germany).

2.10. Statistical analysis

Statistical analysis was performed using SPSS Statistics 19.0 (SPSS Inc., Chicago, IL, USA). Differences between groups were calculated using the *t*-test, ANOVA, χ^2 test, and Mann-Whitney *U* test. Two-tailed *P*-values of < 0.05 were considered statistically significant.

3. Results

3.1. Detection of HAdV and 17 other respiratory pathogens

In total, 1704 paediatric patients ($\leq$ 14 years old) hospitalized with ARI were enrolled in this study; the patients were all from Guangdong Province in southern China, with 74.4% (1268/1704) of patients were from Guangzhou city. A total of 845 (49.6%) patients were infected with one or more of the pathogens of interest. MP (17.8%, 303/1704) and RSV (10.2%, 174/1704) were the most frequently detected pathogens (Fig. 1A). Notably, 151 (8.9%) patients exhibited HAdV infection, such that it was the third most frequently detected pathogen (Fig. 1A). Of the 151 patients with HAdV infection, 108 patients (71.5%) were co-infected with other pathogens; MP (62.9%, 95/151) was the most frequent co-infecting pathogen. HAdV-MP dual infections (without other pathogens) were found in 69 patients.

3.2. HAdV monthly distribution

In this study, HAdV infection occurred year-round, and the incidence peak and trough were in July (27.0%, 66/244) and October (4.4%, 7/158), respectively (Fig. 1B).

3.3. HAdV type distribution

HAdV-positive samples were subjected to molecular typing. Five distinct HAdV types (-3, -7, -21, -55, and -E4) were detected; no samples contained HAdV-14 or -C5 in this study. HAdV-3 (47.0%, 71/151) and HAdV-7 (46.4%, 70/151) were the main epidemic types, while HAdV-21, HAdV-55, HAdV-4 only accounted for 1.3% (2/151), 1.3% (2/151) and 4.0% (6/151), respectively (Fig. 1C).

3.4. Severe and non-severe HAdV infection

The severe illness rate in patients with HAdV infection was 34.4% (52/151). The rate of severe illness was significantly higher in patients with HAdV co-infections (40.7%, 44/108) and in patients with HAdV-MP dual infection (36.2%, 25/69), compared with patients who had single HAdV infection (18.6%, 8/43) ($P < 0.05$) (Fig. 2A). The rate of severe illness significantly differed among patients according to types of HAdV infection ($P < 0.001$). Patients infected with HAdV-7 had the highest rate of severe illness (51.4%, 36/70) (Fig. 2B).

3.5. Clinical feature of HAdV infection

Clinical characteristics of patients with HAdV infection, HAdV-coinfection, and different types of HAdV infection were analysed (Table 1). The median age of patients with HAdV infection was 3.0 [interquartile range (IQR)]: 1.1–5.0) years. No significant differences were found in terms of age and sex distribution between patients according to HAdV infection severity. The proportion of patients with comorbid disease was significantly higher among patients with severe illness (36.5%, 19/52) than among patients with non-severe illness (26.3%, 26/99) ($P = 0.003$) (Table 1). HAdV infection caused abnormalities (exceeding normal values) in six physiological indexes, including procalcitonin (PCT), C-reactive protein (CRP), aspartate aminotransferase (AST), lactate dehydrogenase (LDH), D-dimer, and IL-6 (Table 1). Twelve clinical indexes were significantly higher in patients with severe illness than in patients with non-severe illness ($P \leq 0.019$) (Fig. 3A), while four indexes were significantly lower in patients with

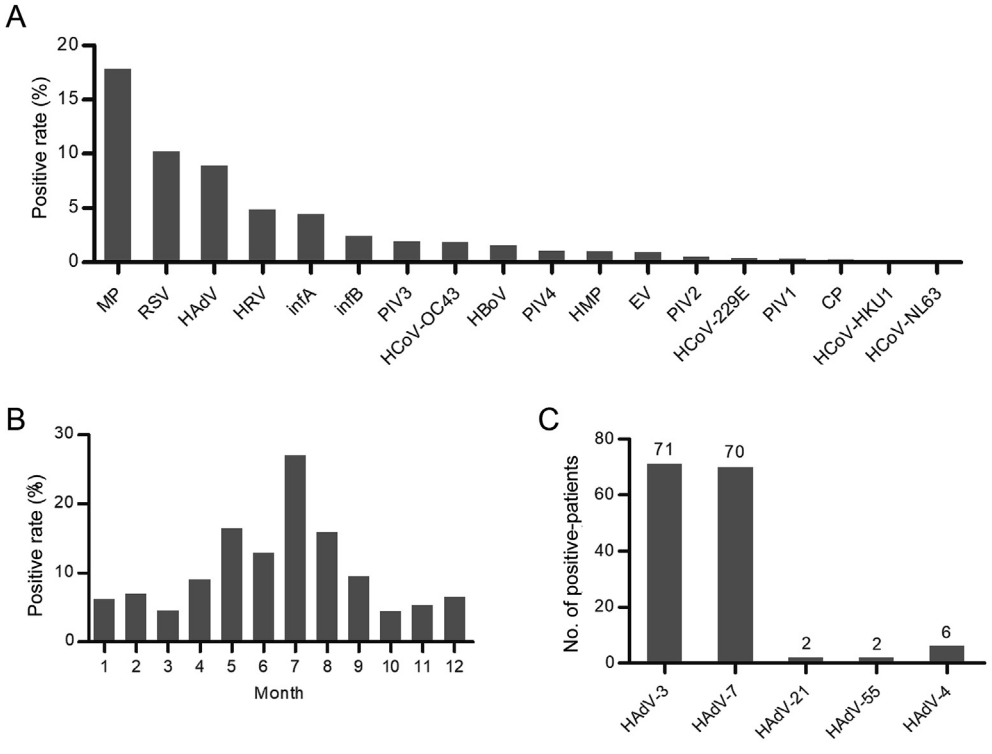

Fig. 1. Human adenovirus distribution in paediatric patients hospitalized with acute respiratory illness in southern China in 2019. **A** Frequency of detection for 18 pathogens. **B** Monthly distribution of HAdV infection. **C** Types of HAdV detected. HAdV, human adenovirus; infA, influenza A virus; infB, influenza B virus; RSV, respiratory syncytial virus; PIV, parainfluenza virus; HMP, human metapneumovirus; HRV, human rhinovirus; EV, enterovirus; HCoV, human coronavirus; HBoV, human bocavirus; MP, *Mycoplasma pneumoniae*; CP, *Chlamydophila pneumonia.*

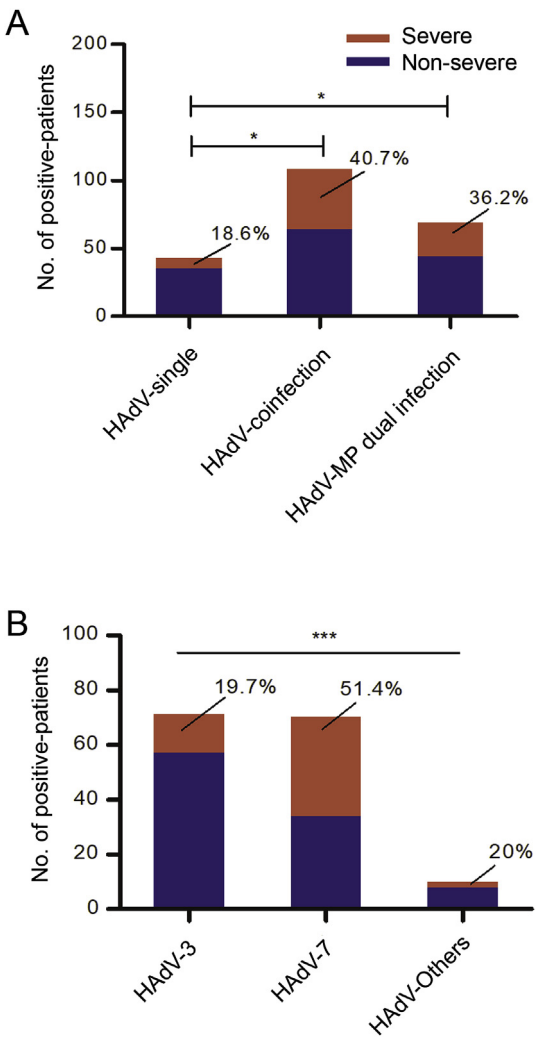

Fig. 2. Severe patient distribution of human adenovirus infection. The distribution of severe illness in patients infected with HAdV-single and co-pathogens (**A**), and in patients infected with different types of HAdV (**B**). Percentage data indicate proportion of patients with severe HAdV infection. Statistical analysis was performed by *t*-test and ANOVA. $^{*}P < 0.05$; $^{***}P < 0.001$.

severe illness ($P \leq 0.007$) (Fig. 3B). There were significant differences in 13 indexes among patients according to HAdV infection type ($P \leq 0.022$) (Fig. 3C and D); 9 of 13 indexes exhibited the highest values in patients with HAdV-7 infection (Fig. 3C).

3.6. Genomes and capsid genes of HAdV-7 isolates

To analyze whether genomes or capsid structural genes differed between HAdV-7 isolates from patients with severe and non-severe illness after different durations of illness, complete genomes of five isolates and capsid protein genes of eight isolates were sequenced and annotated (Table 2). For five complete-genome sequencing isolates, contigs and consensus sequences were acquired by using CLC Genomics Workbench v11.0 based on HAdV-7 strain CQ1198 (accession number JX625134). About 10 million reads were obtained per sample, and resulting in a sequencing depth of 30 × to 500 × coverage of the entire genome. Based on the nucleotide alignment of genomic sequences, the HAdV obtained in this research shared about 99.9% nucleotide identity with the reference genome. Corresponding mutation was labelled as Supplementary Table S3.

3.7. Phylogenetic features of HAdV-7 isolates

Phylogenetic analysis of genomes and capsid structural protein genes of 13 HAdV-7 isolates from patients with severe or non-severe HAdV infection showed that HAdV-7 isolates in this study were closely related to recent isolates from patients in Beijing, Hubei, and Chongqing, as well as two vaccine strains, such that all investigated isolates formed a clade (Fig. 4). The sequence similarity of three capsid protein genes of 13 HAdV-7 isolates was 100%, and the average sequence similarity of the five full-genome isolates was 99.98%. GZ04090 isolated in this study shared 99.46% and 99.43% of the sequence similarities with two vaccine strains (accession no. MN936178 and AY594256) and 99.95% with the previous local epidemic strain HAdV-7 strain CQ1198.

3.8. Proliferation curve of a representative HAdV-7 isolate

Because the genome sequences of HAdV-7 isolates exhibited high similarity, the HAdV-7 isolate GZ04090 was selected for representative analysis of proliferation characteristics, in comparison with the HAdV-3 epidemic strain Guangzhou01. The proliferation curves of the two viruses did not significantly differ ($P > 0.05$) (Fig. 5).

3.9. Cytopathogenesis of a representative HAdV-7 isolate

Cytopathogenicity analyses of HAdV-7 strain GZ04090 and HAdV-3 strain Guangzhou01 were performed using the plaque formation assay method (Fig. 6). Plaques formed by HAdV-7 strain GZ04090 had clearer boundaries (Fig. 6A) and significantly larger sizes than the plaques formed by the HAdV-3 strain ($P < 0.001$; Fig. 6B).

4. Discussion

HAdV is an important respiratory pathogen, which often contributes to regional epidemics and can cause severe pneumonia with potential mortality (Lu et al., 2013; Lion, 2014; Cheng et al., 2018; Ji et al., 2021). This study analysed the infective and pathogenic characteristics of severe HAdV infection in southern China in 2019, with the aim of obtaining the overall profile of the HAdV infection epidemic; it also aimed to provide support for the treatment, prevention, and control of HAdV infection.

In total, 1,704 paediatric patients (aged ≤ 14 years) hospitalized with ARI in southern China were enrolled in this study. HAdV and 17 other respiratory pathogens were tested. Overall, 8.9% of patients exhibited HAdV infection, such that it was the third most frequently detected pathogen (Fig. 1A). This prevalence was higher than in previous reports concerning southern China (Liu et al., 2014). HAdV infection was mainly concentrated in children under five years of age, with a median patient age of three years (Table 1); this population carried the greatest burden of respiratory infection, it comprises the key population for protection (Rodrigues and Groves, 2018; PERCH Study Group, 2019; Ison and Hirsch, 2019). The peak prevalence was in July (27.0%) (Fig. 1B), which was largely consistent with previous findings (Liu et al., 2014).

Clinical statistical analysis of paediatric patients with severe and non-severe HAdV infection in this study revealed that patient age and sex did not significantly differ according to HAdV infection severity. Risk factors for severe illness were comorbid disease, HAdV co-infection, and HAdV type. Comorbid disease has been reported as a risk factor for many viral infections (Pinana et al., 2017; Rodriguez-Fernandez et al., 2017). Pathogen co-infection has also been reported as a risk factor for severe illness. To our knowledge, its mechanism has not been clarified. It has been presumed that a high incidence of co-infection is associated with random events or seasonal overlap of pathogens. The analysis of clinical consequences has mainly been performed from an epidemiological perspective. Because of the lack of direct evidence, the interpretation of viral co-infection has become a major challenge for clinical judgment and treatment (Launes et al., 2012; Scotta et al., 2016). Some recent

Table 1
Clinical characteristics, treatments, and outcomes of patients with human adenovirus infection.

Characteristics[a]	HAdV-Patients (n = 151)	HAdV-positive patients			Patients with HAdV single or co-infection					Patients with different HAdV-types infection			
		Severe (n = 52)	Non-severe (n = 99)	*P*	HAdV-single (n = 43)	HAdV-coinfection (n = 108)	HAdV-MP (n = 69)	*P*[c]	*P*[d]	HAdV-3 (n = 71)	HAdV-7 (n = 70)	HAdV-others (n = 10)	*P*
Male/female	86/65	31/21	55/44	0.73	27/16	59/49	37/32	0.467	0.433	41/30	40/30	5/5	0.897
Age (y)	3.0 (1.1–5.0)	2.9 (1.0–5.0)	3.0 (1.3–5.0)	0.726	2.3 (1.0–4.0)	3.0 (1.5–5.0)	3.3 (2.0–6.0)	**0.046**	**0.005**	3.0 (1.6–4.4)	3.0 (1.0–6.0)	3.1 (0.9–6.0)	0.956
Comorbid disease, n (%)[b]	45 (29.8)	19 (36.5)	26 (26.3)	**0.003**	10 (23.3)	35 (32.4)	17 (24.6)	0.326	0.868	21 (29.6)	22 (31.4)	2 (20)	0.760
Highest temperature (°C)	39.8 (39.2–40.0)	39.8 (39.2–40.1)	39.9 (39.4–40.0)	0.626	40.0 (39.4–40.2)	39.8 (39.2–40.0)	39.8 (39.4–40.0)	0.254	0.645	39.9 (39.2–40.0)	39.8 (39.2–40.1)	39.6 (38.4–40.1)	0.89
Pluse (times/min)	130 (116–140)	130 (122–149)	124 (115–140)	**0.018**	128 (115–136)	130 (118–142)	126 (117–141)	0.142	0.481	126 (116–140)	130 (120–142)	133 (117–146.5)	0.408
Breathe (times/min)	30 (28–36)	36 (30–42)	30 (26–36)	< **0.001**	30 (26–36)	31 (28–36)	30 (28–35)	0.614	0.689	30 (26–36)	32 (29–40)	29.5 (25.0–36.0)	**0.02**
Laboratory findings													
SpO_2 (%),	97.0 (96.0–99.0)	96.0 (90.0–98.0)	98.0 (97.0–99.0)	< **0.001**	97.0 (95.3–98.8)	97 (96–99)	97 (96–99)	0.536	0.372	98.0 (97–99)	97 (93–98)	97.5 (97.0–99.8)	**0.008**
White-cell count —(4–10) × 10^9/L,	7.9 (5.4–11.6)	6.8 (4.8–11.4)	8.8 (5.5–11.8)	0.155	8.7 (5.4–14.5)	7.9 (5.3–11.4)	7.3 (5.3–10.5)	0.437	0.341	9.4 (6.8–13.0)	6.2 (4.44–10.1)	9.6 (7.9–19.3)	**0.001**
neutrophil count —(1.8–8) × 10^9/L	3.9 (2.3–6.4)	4.9 (2.9–6.9)	3.6 (1.9–6.3)	0.1	3.1 (1.6–8.0)	4.2 (2.6–6.3)	3.95 (2.4–6.3)	0.504	0.669	4.6 (2.6–7.6)	3.2 (1.9–5.3)	5.5 (1.5–7.3)	0.059
Lymphocyte count —(0.9–5.2) × 10^9/L	2.6 (1.4–4.2)	1.6 (1.0–3.3)	3.1 (1.8–5.0)	< **0.001**	3.0 (1.9–5.2)	2.5 (1.3–3.7)	2.5 (1.3–3.5)	**0.028**	**0.012**	3.1 (1.9–5.0)	1.9 (1.1–3.7)	2.7 (1.0–8.9)	**0.006**
Red blood cell count —(4.0–5.5) × 10^{12}/L	4.3 (3.9–4.6)	4.1 (3.4–4.5)	4.3 (4.0–4.6)	**0.001**	4.3 (4.0–4.6)	4.2 (3.9–4.6)	4.3 (4.0–4.6)	0.264	0.893	4.3 (4.0–4.6)	4.3 (3.7–4.5)	4.4 (4.0–4.9)	0.243
Haemoglobin —(120–160) g/L	110 (102–118)	108 (96–115)	112 (104–120)	**0.007**	110.5 (101.5–120.0)	110 (102–118)	112 (104–119)	0.972	0.519	112 (103–118)	109 (100–118)	115 (93–128)	0.506
Platelet count Median —(100–400) × 10^9/L	282 (203–367)	254 (180–363)	293 (216–369)	0.215	292 (216–358)	280 (200–379)	261 (202–335)	0.904	0.396	314 (254–405)	234 (159–355)	219 (194–271)	**0.001**
Procalcitonin —(0–0.05) ng/mL	0.35 (0.12–1.25)	0.60 (0.19–2.15)	0.29 (0.09–0.68)	< **0.001**	0.48 (0.17–1.29)	0.29 (0.09–1.22)	0.29 (0.09–1.24)	0.25	0.21	0.21 (0.09–0.56)	0.60 (0.16–2.13)	0.68 (0.53–1.63)	**0.002**
Alanine aminotransferase —(5–40) U/L	14.5 (11.7–19.6)	15.3 (11.1–24.3)	14.05 (11.9–18.3)	0.283	14.0 (11.6–21.9)	14.7 (11.6–19.4)	14.2 (10.4–17.6)	0.869	0.534	13.6 (10.6–16.4)	15.6 (12.5–27.4)	15.0 (9.2–20.0)	**0.011**
C-reactive protein —(0–0.6) mg/dL	1.6 (0.8–3.6)	2.0 (0.9–5.2)	1.4 (0.8–3.0)	0.074	1.4 (0.7–3.7)	1.7 (0.8–3.5)	1.7 (0.9–3.9)	0.695	0.591	1.9 (0.9–3.8)	1.3 (0.6–3.5)	1.4 (0.8–2.2)	0.434
Aspartate aminotransferase —(5–40) U/L	41.8 (31.1–55.0)	55.1 (41.0–70.0)	37.0 (29.9–46.2)	< **0.001**	42.0 (33.7–53.3)	41.0 (30.8–55.9)	41.0 (30.1–52.7)	0.618	0.322	35.0 (29.6–43.9)	50.4 (34.5–70.0)	43.8 (31.3–63.3)	**<0.001**

(*continued on next page*)

Table 1 (*continued*)

Characteristics[a]	HAdV-Patients (n = 151)	HAdV-positive patients			Patients with HAdV single or co-infection					Patients with different HAdV-types infection			
		Severe (n = 52)	Non-severe (n = 99)	*P*	HAdV-single (n = 43)	HAdV-coinfection (n = 108)	HAdV-MP (n = 69)	*P*[c]	*P*[d]	HAdV-3 (n = 71)	HAdV-7 (n = 70)	HAdV-others (n = 10)	*P*
Creatine kinase —(10–190) U/L	74 (52–131)	64 (44–136)	82 (57–131)	0.297	72 (53–121)	76 (51–135)	76 (56–125)	0.774	0.693	65 (46–99)	102 (60–152)	100 (58–251)	**0.022**
Lactate dehydrogenase —(109–255) U/L	347 (277–526)	575 (349–1131)	313 (257–402)	< **0.001**	334 (268–514)	352 (279–530)	331 (279–478)	0.561	0.907	315 (260–398)	470 (295–748)	311 (285–493)	**<0.001**
D-dimer —(68–494) ng/mL	956 (499–2298)	1893 (904–4751)	625 (412–1339)	< **0.001**	939 (527–2390)	961 (444–2289)	881 (441–1950)	0.773	0.953	620 (404–1310)	1483 (639–3409)	881 (356–1348)	**<0.001**
IL-6—(0–5.30) pg/mL	12.31 (5.03–31.45)	20.00 (5.79–58.73)	9.11 (4.85–18.09)	**0.002**	10.97 (4.36–22.37)	14.27 (5.25–39.97)	16.27 (5.29–44.80)	0.334	0.273	9.78 (2.75–20.16)	16.43 (5.03–47.22)	18.58 (5.87–199.44)	0.188
INF-γ—(0–7.42) pg/mL	2.85 (1.09–8.95)	5.27 (1.41–11.36)	2.21 (0.71–4.17)	**0.019**	2.60 (0.67–9.16)	3.24 (1.13–9.11)	3.01 (1.20–11.88)	0.558	0.52	2.84 (0.65–12.97)	2.65 (1.21–7.80)	9.42 (2.82–21.12)	0.397
Treatment and outcome													
Gamma globulin/ plasma therapy, n (%)	91 (60.3)	48 (92.3)	43 (43.4)	< **0.001**	24 (55.8)	67 (62.0)	40 (58.0)	0.581	0.847	34 (47.9)	52 (74.3)	5 (50)	**0.005**
Oxygen therapy, n (%)	65 (43.0)	45 (86.5)	20 (20.2)	< **0.001**	14 (32.6)	51 (46.8)	31 (44.9)	0.106	0.236	21 (29.6)	41 (58.6)	3 (30)	**0.002**
Length of hospital stay (d)	6.0 (5.0–11.0)	12.5 (9.3–17.8)	5.0 (4.0–7.0)	< **0.001**	6.0 (4.0–7.0)	7.0 (5.0–12.0)	7.0 (5.0–11.0)	**0.006**	**0.028**	6.0 (4.0–7.0)	8.0 (6.0–14.0)	6.0 (4.0–7.8)	**0.001**

Data are median (IQR) in each group, except where indicated otherwise. Bold fonts are used to indicate statistical values with significant differences.
Statistical analysis was performed by χ^2 test and Mann-Whitney *U* test.

[a] Index name = Index—(normal value range) and measurement unit, except where indicated otherwise.

[b] Including anemia, allergies, postoperative immunosuppression, congenital heart disease, fava bean disease, eczema, premature birth, malnutrition.

[c] Comparison of index distribution between HAdV-coinfected patients and HAdV-single infected patients.

[d] Comparison of index distribution between HAdV-MP dual infected patients and HAdV-single infected patients.

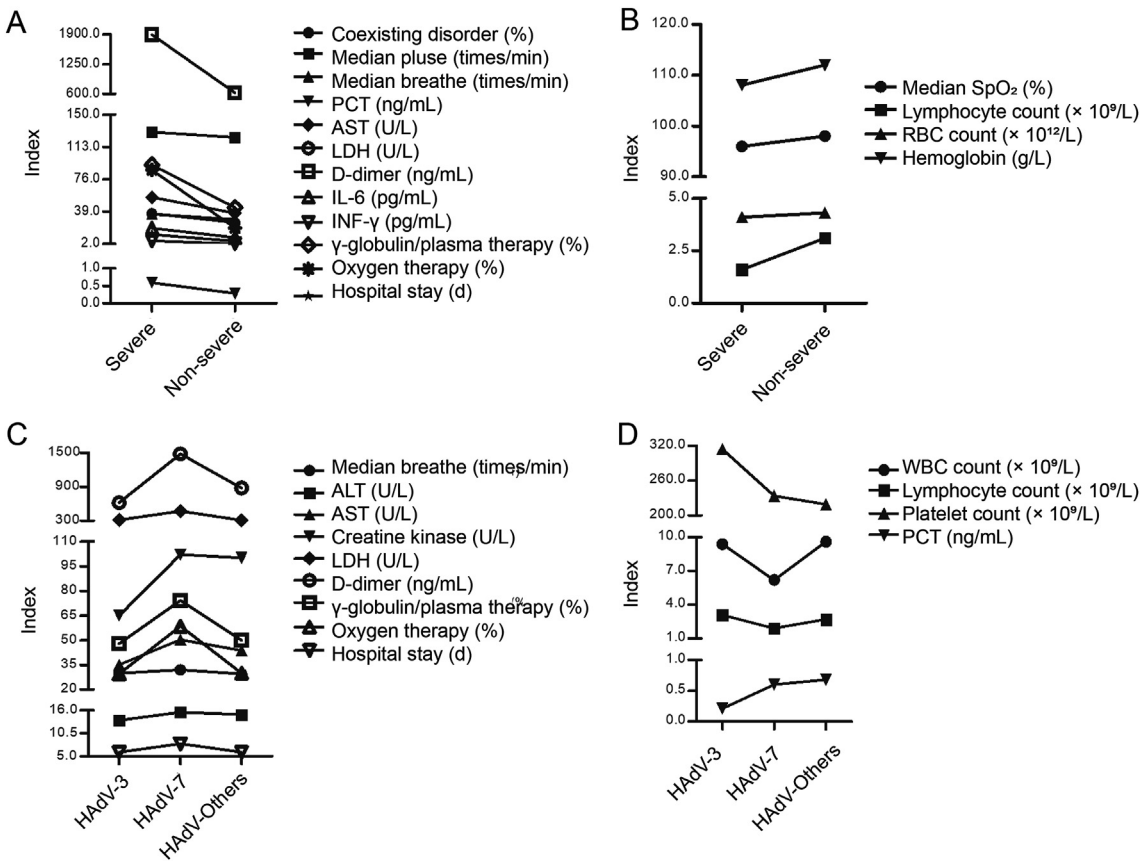

Fig. 3. Clinical manifestations in patients with human adenovirus infection. Differential distributions of clinical indexes in patients with severe and non-severe HAdV infection, and in patients with different types of HAdV infection were analysed ($P < 0.05$). Clinical indexes were significantly higher (**A**), or lower (**B**) in patients with severe HAdV infection than in patients with non-severe HAdV infection ($P \leq 0.019$). Clinical indexes demonstrated the highest values in patients with HAdV-7 infection (**C**) or not (**D**) ($P \leq 0.022$). Data are shown as median values except for percentages in clinical indexes. Statistical analysis was performed by Mann-Whitney *U* test and ANOVA. WBC, white blood cell; RBC, red blood cell; PCT, procalcitonin; CRP, C-reactive protein; AST, aspartate aminotransferase; LDH, lactate dehydrogenase; ALT, alanine aminotransferase.

Table 2
Sequencing and annotation data regarding human adenovirus type 7 isolates from paediatric patients with severe and non-severe illness after different durations of illness in southern China in 2019.

Patient	Isolation month	Gene or genome	Genbank accession number
Severe-pneumonia isolate			
GZ02004	2	Hexon/Fiber/Penton base	MT895675/MT895661/MT895689
GZ05043	5	Hexon/Fiber/Penton base	MT895671/MT895656/MT895686
GZ06189	6	Hexon/Fiber/Penton base	MT895670/MT895655/MT895685
GZ07210	7	Hexon/Fiber/Penton base	MT895672/MT895657/MT895687
GZ08080	8	Hexon/Fiber/Penton base	MT895669/MT895654/MT895684
GZ04090	4	genome	MT920215
GZ04160	4	genome	MT941567
GZ06091	6	genome	MT941568
GZ06173	6	genome	MT950360
GZ07010	7	genome	MT950361
Non-severe pneumonia isolate			
GZ03130	3	Hexon/Fiber/Penton base	MT895674/MT895660/MT895682
GZ04031	4	Hexon/Fiber/Penton base	MT895673/MT895659/MT895688
GZ04146	4	Hexon/Fiber/Penton base	MT895668/MT895658/MT895681

co-infection studies have shown that a virus-infected host cell can hinder co-infection by other viruses. Moreover, viruses affect each other during co-infection, altering virus replication ability (Pinky and Dobrovolny, 2016; Opatowski et al., 2018) in relation to resource competition among viruses (Pinky and Dobrovolny, 2017; Smith, 2018). However, interactions of viruses are reportedly influenced by virus type and the local microenvironment, which may lead to mutually reinforcing outcomes. For example, co-infection by ssDNA and dsDNA viruses is more efficient than infection with a single ssDNA virus alone (Diaz-Munoz, 2017). In this study, we found that patients with HAdV-MP dual infection were more likely to develop severe illness. It has been suggested that both MP and HAdV can reduce cilia function and cause severe respiratory mucosal damage (Kajon et al., 2003; Kotha et al., 2015; Chaudhry et al., 2016; Prince et al., 2018), which may increase respiratory tract susceptibility and produce cytokine storm. Further research in this area will provide important insights for clinical treatment of patients with HAdV-MP co-infection.

HAdV is a DNA virus with a generally conserved genome. In this study, no significant phylogenetic difference between isolates according to HAdV infection severity was found. Therefore, viral genome variation may not be a key factor for the high incidence of HAdV-7 infection. Our study in 2020 revealed low levels of herd immunity against HAdV-3 and -7 in children in southern China (Tian et al., 2020), which may be important factors for the high incidences of HAdV-7 and -3 infections. The current and previous findings also suggest that there is a critical need for monitoring and control of HAdV infection, as well as development of a HAdV vaccine.

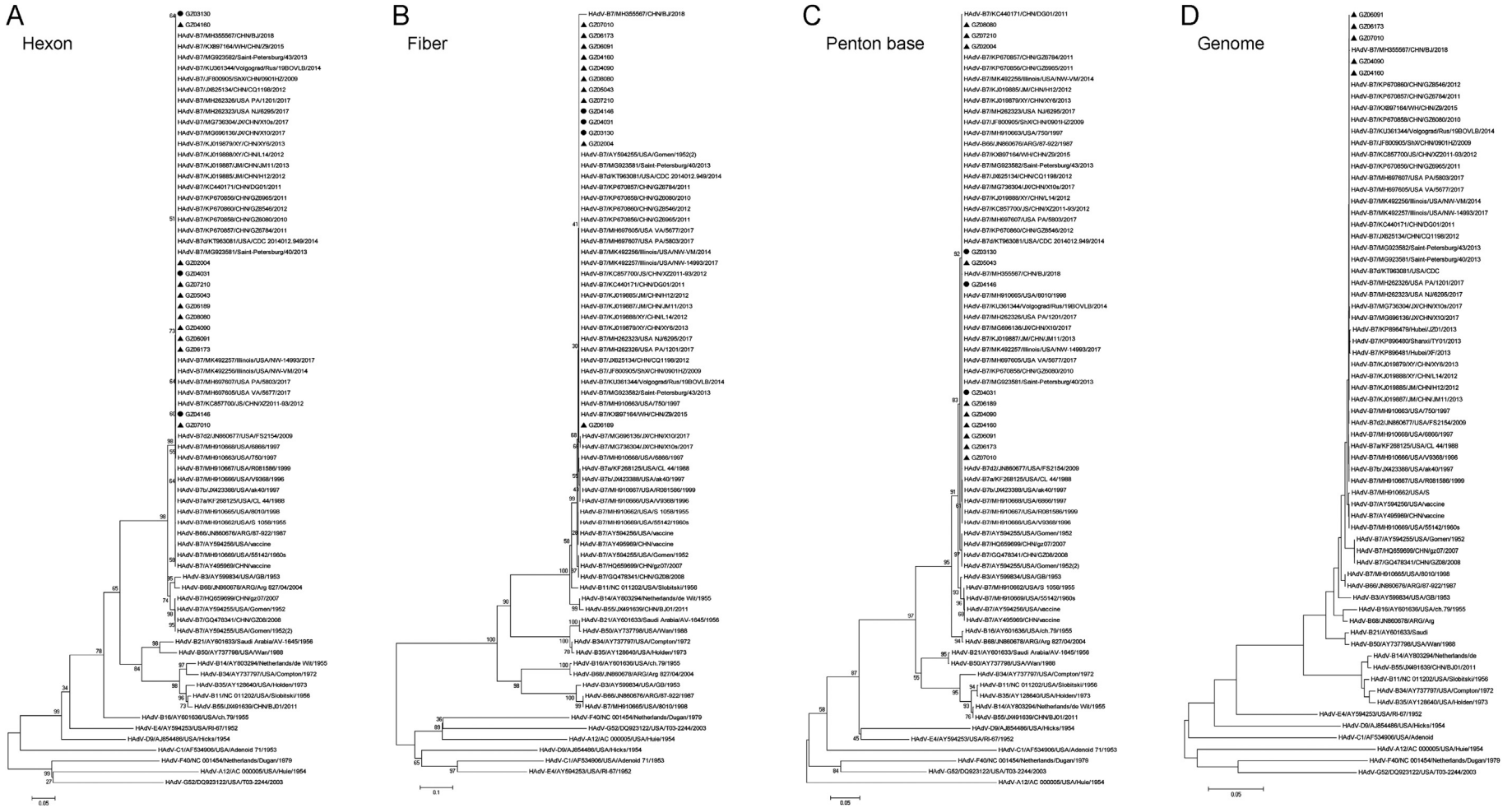

Fig. 4. Phylogenetic analysis of human adenovirus type 7 isolates. Thirteen HAdV-7 isolates were subjected to nucleotide sequencing analyses of the hexon (**A**), fiber (**B**), and penton base (**C**) genes, while five HAdV-7 isolates were subjected to whole genome analyses (**D**), to determine their phylogenetic relationships using the neighbour-joining method with 1000 bootstrap replicates implemented in MEGA 5.0 software. For reference, taxon names include genome type, corresponding GenBank accession number, country of isolation, strain name, and year of isolation. Strains of HAdV-7 isolated from patients with severe and non-severe illness in this study are marked with "▲" and "●", respectively.

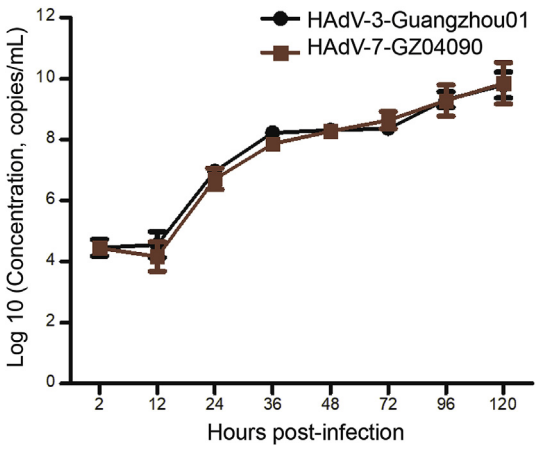

Fig. 5. DNA proliferation curves of a representative human adenovirus type 7 isolate and the reference human adenovirus type 3 strain Guangzhou01. Cells infected with the selected viruses were harvested at 2, 12, 24, 36, 48, 72, 96, and 120 h post-infection. Genome copy numbers were determined by qPCR. Each experiment was repeated independently three times, and the mean values and standard deviations are shown. Statistical analysis was performed by Mann-Whitney *U* test. No significant differences were found ($P > 0.05$).

Comparison of proliferation and cytopathogenesis properties between the representative HAdV-7 strain GZ04090 and the HAdV-3 epidemic strain Guangzhou01 revealed no significant differences. However, HAdV-7 exhibited greater virulence and infectivity than HAdV-3, consistent with the findings by Fu et al., (2019). These differences may play an important role in the high incidence of severe illness in patients with HAdV-7 infection.

In this study, we analysed the clinical features, physiological indexes, treatments, and outcomes of HAdV infection. Significant differences were found in various clinical indexes upon comparison of clinical data between patients according to HAdV infection severity and HAdV types. These data will help to improve the overall understanding of HAdV infection. In particular, differences in these indexes among patients with severe HAdV infection may provide important reference data for patient treatment.

This study had a few limitations. In particular, we only analysed paediatric inpatients and did not include outpatients. Furthermore, we only included patients from two hospitals. Therefore, the findings may not be fully representative of HAdV infection, and the results should be interpreted cautiously.

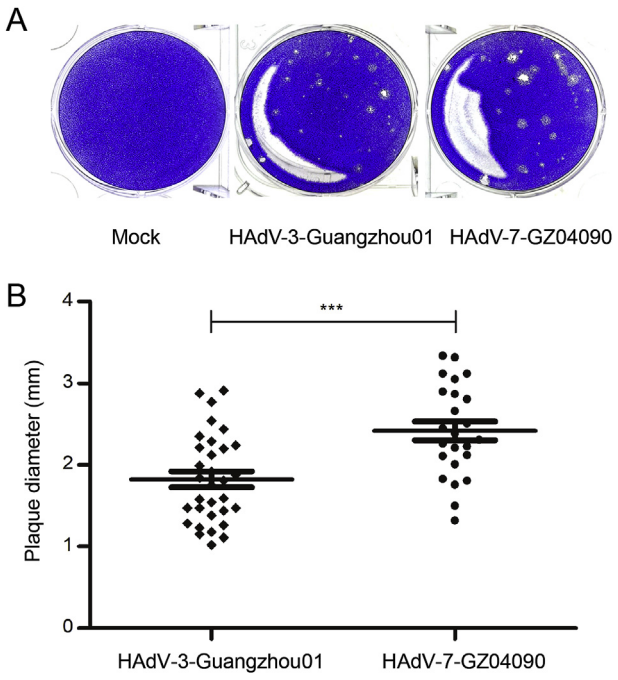

Fig. 6. Plaque formation (**A**) and size distribution (**B**) of a representative human adenovirus type 7 isolate and the reference human adenovirus type 3 strain Guangzhou01. Plaque plates were incubated and stained with crystal violet for 13 days in six-well culture plates. Data are shown as mean values with standard deviations. Statistical analysis was performed by Mann-Whitney *U* test. ***$P < 0.001$.

5. Conclusions

In conclusion, this study analysed HAdV infection, clinical features, and risk factors for severe illness in hospitalized children with ARI in southern China in 2019. The findings showed that HAdV co-infection and comorbid disease were important patient-related risk factors for severe illness; high virulence and infectivity of HAdV-7 were important virus-related risk factors for severe illness. The results of this study offer important reference data for management of this HAdV epidemic, which also offer support for subsequent treatment, control, and prevention of HAdV infection.

Data availability

All data generated or analysed during this study are included in this published article and its supplementary information files. The complete and partial genomes of HAdV-7 isolates identified in this study were deposited in GenBank under the accession numbers: MT920215, MT941567–MT941568, MT950360–MT950361, MT895654–MT895661, MT895668–MT895675, MT895681–MT895682, and MT895684–MT895689.

Ethics statement

The study was approved by the First Affiliated Hospital of Guangzhou Medical University Ethics Committee. Next of kin, caretakers, or guardians provided written informed consent for participation in the study on behalf of all minors/children.

Author contributions

Wenkuan Liu: conceptualization, formal analysis, funding acquisition, methodology, writing - original draft. Shuyan Qiu: data curation, formal analysis, investigation, writing - original draft. Li Zhang: data curation, investigation, visualization. Hongkai Wu: methodology, software. Xingui Tian: investigation, visualization. Xiao Li: methodology, visualization. Duo Xu: data curation, investigation. Jing Dai: investigation, methodology. Shujun Gu: data curation, investigation. Qian Liu: conceptualization, formal analysis, funding acquisition, resources, writing - reviewing and editing. Dehui Chen: methodology, project administration, resources, supervision, validation, writing - reviewing and editing. Rong Zhou: conceptualization, funding acquisition, project administration, writing - reviewing and editing.

Conflict of interest

The authors declare that they have no known competing financial interests or personal relationships that could have appeared to influence the work reported in this paper.

Acknowledgments

We thank the patients for their participation in this study. We also thank Yinghua Zhou and Jing Ma for their technical assistance. This study was supported by the Guangzhou Science and Technology

Program-Zhongnanshan Medical Foundation of Guangdong Province (202102010359-ZNSA-2020003); the Emergency Key Program of Guangzhou Laboratory (EKPG21-13); the National Natural Science Foundation of China (81970003, 31900877); the Natural Science Foundation of Guangdong Province of China (2018A030310401); Guangdong-Hong Kong-Macao Joint Laboratory of Respiratory Infectious Disease (GHMJLRID-Z-202109); and the Special Project for COVID-19 Prevention and Control of Zhongnanshan Medical Foundation of Guangdong Province (ZNSA-2020012). The funders had no input in the study design, data collection, or interpretation, or the decision to submit the work for publication.

Appendix A. Supplementary data

Supplementary data to this article can be found online at https://doi.org/10.1016/j.virs.2022.01.010.

References

Chaudhry, R., Ghosh, A., Chandolia, A., 2016. Pathogenesis of Mycoplasma pneumoniae: an update. Indian J. Med. Microbiol. 34, 7–16.
Chen, S.Y., Liu, W., Xu, Y., Qiu, S., Chen, Y., Tian, X., Zhou, R., 2020. Epidemiology and genetic variabilities of human adenovirus type 55 reveal relative genome stability across time and geographic space in China. Front. Microbiol. 11, 606195.
Cheng, Z., Yan, Y., Jing, S., Li, W.G., Chen, W.W., Zhang, J., Li, M., Zhao, S., Cao, N., Ou, J., Zhao, S., Wu, X., Cao, B., Zhang, Q., 2018. Comparative genomic analysis of Re-emergent human adenovirus type 55 pathogens associated with adult severe community-acquired pneumonia reveals conserved genomes and capsid proteins. Front. Microbiol. 9, 1180.
Dean, P., Florin, T.A., 2018. Factors associated with pneumonia severity in children: a systematic review. J Pediatric Infect Dis Soc 7, 323–334.
del Rio, C., Guarner, J., 2010. The 2009 influenza A (H1N1) pandemic: what have we learned in the past 6 months. Trans. Am. Clin. Climatol. Assoc. 121, 128–137 discussion 138–140.
Diaz-Munoz, S.L., 2017. Viral coinfection is shaped by host ecology and virus-virus interactions across diverse microbial taxa and environments. Virus Evol 3, vex011.
Fu, Y., Tang, Z., Ye, Z., Mo, S., Tian, X., Ni, K., Ren, L., Liu, E., Zang, N., 2019. Human adenovirus type 7 infection causes a more severe disease than type 3. BMC Infect. Dis. 19, 36.
Greber, U.F., Flatt, J.W., 2019. Adenovirus entry: from infection to immunity. Annu Rev Virol 6, 177–197.
Ismail, A.M., Lee, J.S., Lee, J.Y., Singh, G., Dyer, D.W., Seto, D., Chodosh, J., Rajaiya, J., 2018. Adenoviromics: mining the human adenovirus species D genome. Front. Microbiol. 9, 2178.
Ison, M.G., Hirsch, H.H., 2019. Community-acquired respiratory viruses in transplant patients: diversity, impact, unmet clinical needs. Clin. Microbiol. Rev. 32, e00042–19.
Ji, T., Li, L., Li, W., Zheng, X., Ye, X., Chen, H., Zhou, Q., Jia, H., Chen, B., Lin, Z., Chen, H., Huang, S., Seto, D., Chen, L., Feng, L., 2021. Emergence and characterization of a putative novel human adenovirus recombinant HAdV-C104 causing pneumonia in Southern China. Virus Evol 7, veab018.
Kajon, A.E., Gigliotti, A.P., Harrod, K.S., 2003. Acute inflammatory response and remodeling of airway epithelium after subspecies B1 human adenovirus infection of the mouse lower respiratory tract. J. Med. Virol. 71, 233–244.
Kotha, P.L., Sharma, P., Kolawole, A.O., Yan, R., Alghamri, M.S., Brockman, T.L., Gomez-Cambronero, J., Excoffon, K.J., 2015. Adenovirus entry from the apical surface of polarized epithelia is facilitated by the host innate immune response. PLoS Pathog. 11, e1004696.
Launes, C., de-Sevilla, M.F., Selva, L., Garcia-Garcia, J.J., Pallares, R., Munoz-Almagro, C., 2012. Viral coinfection in children less than five years old with invasive pneumococcal disease. Pediatr. Infect. Dis. J. 31, 650–653.
Lion, T., 2014. Adenovirus infections in immunocompetent and immunocompromised patients. Clin. Microbiol. Rev. 27, 441–462.
Liu, W.K., Liu, Q., Chen, de H., Liang, H.X., Chen, X.K., Chen, M.X., Qiu, S.Y., Yang, Z.Y., Zhou, R., 2014. Epidemiology of acute respiratory infections in children in guangzhou: a three-year study. PLoS One 9, e96674.
Lu, M.P., Ma, L.Y., Zheng, Q., Dong, L.L., Chen, Z.M., 2013. Clinical characteristics of adenovirus associated lower respiratory tract infection in children. World J Pediatr 9, 346–349.
Lynch 3rd, J.P., Kajon, A.E., 2016. Adenovirus: epidemiology, global spread of novel serotypes, and advances in treatment and prevention. Semin. Respir. Crit. Care Med. 37, 586–602.
Opatowski, L., Baguelin, M., Eggo, R.M., 2018. Influenza interaction with cocirculating pathogens and its impact on surveillance, pathogenesis, and epidemic profile: a key role for mathematical modelling. PLoS Pathog. 14, e1006770.
Paules, C.I., Eisinger, R.W., Marston, H.D., Fauci, A.S., 2017. What recent history has taught us about responding to emerging infectious disease threats. Ann. Intern. Med. 167, 805–811.
Pinana, J.L., Madrid, S., Perez, A., Hernandez-Boluda, J.C., Gimenez, E., Terol, M.J., Calabuig, M., Navarro, D., Solano, C., 2018. Epidemiologic and clinical characteristics of coronavirus and bocavirus respiratory infections after allogeneic stem cell transplantation: a prospective single-center study. Biol. Blood Marrow Transplant. 24, 563–570.
Pinky, L., Dobrovolny, H.M., 2016. Coinfections of the respiratory tract: viral competition for resources. PLoS One 11, e0155589.
Pinky, L., Dobrovolny, H.M., 2017. The impact of cell regeneration on the dynamics of viral coinfection. Chaos 27, 063109.
Pneumonia Etiology Research for Child Health Study G, 2019. Causes of severe pneumonia requiring hospital admission in children without HIV infection from Africa and Asia: the PERCH multi-country case-control study. Lancet 394, 757–779.
Prince, O.A., Krunkosky, T.M., Sheppard, E.S., Krause, D.C., 2018. Modelling persistent Mycoplasma pneumoniae infection of human airway epithelium. Cell Microbiol. 20.
Prusinkiewicz, M.A., Mymryk, J.S., 2019. Metabolic reprogramming of the host cell by human adenovirus infection. Viruses 11, 141.
Radke, J.R., Cook, J.L., 2018. Human adenovirus infections: update and consideration of mechanisms of viral persistence. Curr. Opin. Infect. Dis. 31, 251–256.
Rodrigues, C.M.C., Groves, H., 2018. Community-acquired pneumonia in children: the challenges of microbiological diagnosis. J. Clin. Microbiol. 56, e01318–17.
Rodriguez-Fernandez, R., Tapia, L.I., Yang, C.F., Torres, J.P., Chavez-Bueno, S., Garcia, C., Jaramillo, L.M., Moore-Clingenpeel, M., Jafri, H.S., Peeples, M.E., Piedra, P.A., Ramilo, O., Mejias, A., 2017. Respiratory syncytial virus genotypes, host immune profiles, and disease severity in young children hospitalized with bronchiolitis. J. Infect. Dis. 217, 24–34.
Sandkovsky, U., Vargas, L., Florescu, D.F., 2014. Adenovirus: current epidemiology and emerging approaches to prevention and treatment. Curr. Infect. Dis. Rep. 16, 416.
Scott, M.K., Chommanard, C., Lu, X., Appelgate, D., Grenz, L., Schneider, E., Gerber, S.I., Erdman, D.D., Thomas, A., 2016. Human adenovirus associated with severe respiratory infection, Oregon, USA, 2013-2014. Emerg. Infect. Dis. 22, 1044–1051.
Scotta, M.C., Chakr, V.C., de Moura, A., Becker, R.G., de Souza, A.P., Jones, M.H., Pinto, L.A., Sarria, E.E., Pitrez, P.M., Stein, R.T., Mattiello, R., 2016. Respiratory viral coinfection and disease severity in children: a systematic review and meta-analysis. J. Clin. Virol. 80, 45–56.
Smith, A.M., 2018. Host-pathogen kinetics during influenza infection and coinfection: insights from predictive modeling. Immunol. Rev. 285, 97–112.
Tamura, K., Peterson, D., Peterson, N., Stecher, G., Nei, M., Kumar, S., 2011. MEGA5: molecular evolutionary genetics analysis using maximum likelihood, evolutionary distance, and maximum parsimony methods. Mol. Biol. Evol. 28, 2731–2739.
Tian, X., Fan, Y., Wang, C., Liu, Z., Liu, W., Xu, Y., Mo, C., You, A., Li, X., Rong, X., Zhou, R., 2021. Seroprevalence of neutralizing antibodies against six human adenovirus types indicates the low level of herd immunity in young children from guangzhou, China. Virol. Sin. 36, 373–381.
Wiersinga, W.J., Rhodes, A., Cheng, A.C., Peacock, S.J., Prescott, H.C., 2020. Pathophysiology, transmission, diagnosis, and treatment of coronavirus disease 2019 (COVID-19): a review. JAMA 324, 782–793.
Zhang, J., Kang, J., Dehghan, S., Sridhar, S., Lau, S.K.P., Ou, J., Woo, P.C.Y., Zhang, Q., Seto, D., 2019. A survey of recent adenoviral respiratory pathogens in Hong Kong reveals emergent and recombinant human adenovirus type 4 (HAdV-E4) circulating in civilian populations. Viruses 11, 129.
Zhang, Q., Su, X., Gong, S., Zeng, Q., Zhu, B., Wu, Z., Peng, T., Zhang, C., Zhou, R., 2006. Comparative genomic analysis of two strains of human adenovirus type 3 isolated from children with acute respiratory infection in southern China. J. Gen. Virol. 87, 1531–1541.
Zhu, N., Zhang, D., Wang, W., Li, X., Yang, B., Song, J., Zhao, X., Huang, B., Shi, W., Lu, R., Niu, P., Zhan, F., Ma, X., Wang, D., Xu, W., Wu, G., Gao, G.F., Tan, W., China Novel Coronavirus, I., Research, T., 2020. A novel coronavirus from patients with pneumonia in China, 2019. N. Engl. J. Med. 382, 727–733.